Spatial impulse responses from a flexible baffled circular piston

Ronald M. Aarts[a)]
Philips Research Europe HTC 36 (WO-02), NL-5656 AE Eindhoven, The Netherlands

Augustus J. E. M. Janssen
Technical University Eindhoven, EURANDOM and Department Electrical Engineering, Den Dolech 2, LG-1, P.O. Box 513, NL-5600 MB Eindhoven, The Netherlands

The theory of orthogonal polynomial (Zernike) expansions of functions on a disk, as used in the diffraction theory of optical aberrations, is applied to obtain (semi-) analytical expressions for the spatial impulse responses arising from a non-uniformly moving, baffled, circular piston. These expressions are in terms of the expansion coefficients of the non-uniformity and the responses of the orthogonal expansion functions. The latter impulse responses have a closed form as finite series involving the Legendre functions and the sinc function. The method is compared with a similar method, proposed by P. R. Stepanishen [J. Acoust. Soc. Am. **70**, 1176–1181 (1981)] where zeroth order orthogonal Bessel functions, rather than Zernike polynomials, are used as expansion functions.
© 2011 Acoustical Society of America. [DOI: 10.1121/1.3562558]

I. INTRODUCTION

The calculation of the sound pressure occurring in loudspeakers and ultrasound due to a vibrating, baffled, planar piston is often done by using the spatial impulse response approach as can be found in Refs. 1–7 for instance. After computation of the spatial impulse responses, the spatial sound pressure is obtained by convolving the impulse responses with the piston velocity waveform which can be any function of time. The required impulse responses comprise a spatial source velocity distribution v, to be called velocity profile in the sequel, the non-uniformity of which makes the computation of the responses a challenging problem. In Ref. 2, Sec. II C and Ref. 3, Sec. I, Harris presents ample review material and history on the spatial impulse response approach, with due attention to the problem of (analytically) computing impulse responses, in particular for circular pistons. The calculation procedures for impulse responses of (apodized) pistons of different shapes were considered in Ref. 4. A rather recent survey on transient acoustics with many details for the circular and rectangular (unapodized) piston can be found in Ref. 5. In Ref. 6, a number of numerically oriented approaches for time-harmonic pressure calculations from spatial impulse responses in the case of a circular piston with uniform velocity profile are compared and combined using a grid sectoring method.

In this paper, a (semi-) analytic method for the computation of the spatial impulse responses arising from a baffled, circular piston with non-uniform piston velocity profile v is presented. A general, radially symmetric, velocity profile $v(\sigma)$, vanishing outside $\sigma \leq a$ (with a the piston radius and σ the radial distance from the origin in the piston plane) is developed into the basis functions $R_{2n}^0(\sigma/a) = P_n(2(\sigma/a)^2 - 1)$, $n = 0, 1, \ldots$, where P_n is the Legendre polynomial of degree n. It will be shown that the impulse responses due to a single basis function have an explicit, finite-series expression in terms of the Legendre functions and the sinc function. The spatial impulse response due to v is then obtained by a linear combination of the appropriate basis functions using the expansion coefficients of v.

Zernike polynomial expansions were used by the authors[8–10] recently in the field of acoustic radiation for the calculation of the pressure and related quantities. In Refs. 8 and 9, this has been done for the on-axis sound pressure, the pressure at the edge, the reaction on the radiator, the far field and the directivity, and the total radiated power. In Ref. 10, the sound field due to a harmonically excited, flexible, spherical cap on a rigid sphere is computed using expansions into appropriately warped Zernike polynomials of axially symmetric velocity profiles on the cap. The Refs. 8 and 9 were, among other things, aimed at systemizing and generalizing the analytic results as obtained by Greenspan in Ref. 11 on piston radiation. Greenspan's results in Ref. 11, Sec. VI on transient responses, however, were not considered yet and it is one of the aims of the present paper to find out what can be done in this respect.

The approach used in the present paper is to be compared with the one presented in Ref. 7, Sec. II, where, as a special case of the theory developed in Ref. 7, Sec. I, the chosen basis functions are of the form $J_0(\alpha_n\sigma/a)$, $0 \leq \sigma \leq a$, with $\alpha_0 = 0$ and α_n the nth positive zero of the Bessel function J_0 of the first kind and order 0. The impulse responses corresponding to the terms $J_0(\alpha_n\sigma/a)$ are shown in Ref. 7 to have a representation as an infinite series involving the product of two Bessel functions and the sinc function. Hence, this also yields a (semi-) analytic method to compute impulse responses in the case of flexible velocity profiles on the piston. However, the series for the impulse responses

[a)]Author to whom correspondence should be addressed. Also at: Technical University Eindhoven, Department EE, Den Dolech 2, PT3.23, P.O. Box 513, NL-5600 MB Eindhoven, The Netherlands. Electronic mail: ronald.m.aarts@philips.com

have infinitely many terms. Furthermore, the expansion coefficients with respect to the Bessel basis functions will be shown to be more awkward in various respects than those that arise when the $R_{2n}^0(\sigma/a)$ are chosen as basis functions. Also, see Ref. 12 where the $R_{2n}^0(\sigma/a)$ are compared with respect to coefficient decay with a set of basis functions of the Bessel type slightly different from the one used in Ref. 7.

In Sec. II, the geometry, notations, and basic formulas are presented. In Sec. III, the proof of the main result of this paper, the finite-series expression in Eqs. (23) and (24) for the impulse responses due to any of the $R_{2n}^0(\sigma/a)$, $\sigma \leq a$ is presented. In Sec. IV, the method is shown to generalize Greenspan's result on the impulse responses due to low-order parabolic velocity profiles [of the form $(1-(\sigma/a)^2)^l$, $\sigma \leq a$], some plots of impulse responses (using a Mathematica code presented in Appendix C) are shown, and the method is compared with the one presented in Ref. 7, Sec. II. In Sec. V, conclusions and directions for further research are presented.

II. GEOMETRY, NOTATIONS, AND BASIC FORMULAS

In this section, the basic formulas as well as the geometry and notations are presented. The radiated pressure, due to a harmonic excitation $\exp(i\omega t)$, with ω the radian frequency, of the harmonically vibrating flat surface S, a disk of radius a around the origin, is given by the Rayleigh integral as

$$p(\underline{r}, \omega) = \frac{i\rho_0 ck}{2\pi} \int_S v(\underline{r}_s) \frac{e^{-ikr'}}{r'} dS, \tag{1}$$

in which the time variable t and the factor $\exp(i\omega t)$ have been suppressed. In Eq. (1), ρ_0 is the density of the medium, c is the speed of sound in the medium, and $k = \omega/c$ is the wave number. Furthermore, $\underline{r}$ is a field point in the half space in front of the baffle containing S, $\underline{r}_s$ is a point on the surface S, and $r' = |\underline{r} - \underline{r}_s|$ is the distance between $\underline{r}$ and $\underline{r}_s$. Finally, $v(\underline{r}_s)$ is the normal component of the velocity on the surface S at $\underline{r}_s$, and the average velocity V_s is given by

$$V_s = \frac{1}{\pi a^2} \int_S v(\underline{r}_s) dS. \tag{2}$$

It is assumed that $v(\underline{r}_s) = v(\sigma)$ is radially symmetric. See Fig. 1 for geometry and notations.

The velocity potential $\phi(\underline{r}, \omega)$ is given by

$$\phi(\underline{r}, \omega) = \frac{1}{i\rho_0 ck} p(\underline{r}, \omega) = \frac{1}{2\pi} \int_S v(\underline{r}_s) \frac{e^{-ikr'}}{r'} dS. \tag{3}$$

The velocity waveform of the field point $\underline{r}$ due to the harmonic excitation $\exp(i\omega t)$ is given as $\phi(\underline{r}, \omega)\exp(i\omega t)$ and can be regarded as the output of a time-invariant linear system with impulse response function $h(t; \underline{r})$. Hence, $\phi(\underline{r}, \omega)$ equals the Fourier transform $\int_{-\infty}^{\infty} \exp(-i\omega t)h(t; \underline{r})dt$ of $h(t; \underline{r})$ with respect to t. Therefore, from Eq. (3), the impulse response $h(t; \underline{r})$ at time $t > 0$ and at field point $\underline{r}$ is obtained in the manner of Ref. 7, Sec. I or Ref. 3, Sec. I B by inverse Fourier transformation of the right-hand side of Eq. (3) with respect to k and choosing appropriate polar coordinates in the piston plane while changing integration variables appropriately. For
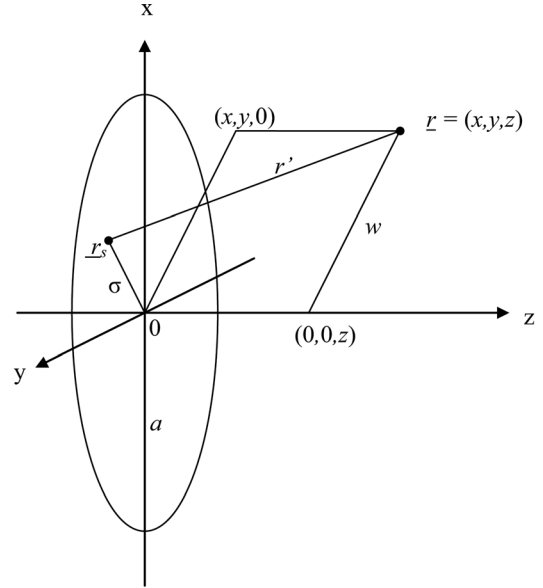
$$\underline{r}_s = (x_s, y_s, 0), \quad \sigma = |\underline{r}_s| = (x_s^2 + y_s^2)^{1/2},$$

$$\underline{r} = (x, y, z), \quad w = (x^2 + y^2)^{1/2}, \quad r' = |\underline{r} - \underline{r}_s|.$$

FIG. 1. Geometry and notations. The piston is surrounded by an infinite rigid baffle.

the readers' convenience, the argument used in Ref. 7, Sec. I is briefly repeated in Appendix A. The result is that

$$h(t; \underline{r}) = \frac{c}{\pi V_s} H(ct - z)$$
$$\times \int_0^A v[(w^2 + R^2(t; z) - 2wR(t; z) \cos \alpha)^{1/2}] d\alpha, \tag{4}$$

in which H is the Heaviside step function

$$H(x) = 0, \ x < 0; \ H(0) = 1/2; \ H(x) = 1, \ x > 0, \tag{5}$$

and

$$R(t; z) = \sqrt{c^2 t^2 - z^2}, \quad ct \geq z, \tag{6}$$

while

$$A = \begin{cases} 0 & , |w - R(t; z)| > a, \\ \arccos\left(\dfrac{w^2 + R^2(t; z) - a^2}{2wR(t; z)}\right) & , |w - R(t; z)| < a < w + R(t; z), \\ \pi & , w + R(t; z) < a. \end{cases} \tag{7}$$

The velocity profiles considered in this paper are square integrable over S and radially symmetric while they vanish for $|\underline{r}_s| > a$. These v's admit a representation,

$$v(\sigma) = V_s \sum_{n=0}^{\infty} u_n R_{2n}^0(\sigma/a), \ 0 \leq \sigma \leq a, \tag{8}$$

in which V_s is given in Eq. (2) and u_n are scalar coefficients with $u_0 = 1$. In Eq. (8), R_{2n}^0 is the radially symmetric Zernike circle polynomial of degree $2n$, given by

J. Acoust. Soc. Am., Vol. 129, No. 5, May 2011

R. M. Aarts and A. J. Janssen: Spatial impulse responses   2953

$$R^0_{2n}(\rho) = P_n(2\rho^2 - 1), \quad 0 \le \rho \le 1, \tag{9}$$

with P_n the Legendre polynomial of degree n, see Ref. 13, Chap. 22.

III. PROOF OF THE MAIN RESULT

In this section, the main result of this paper is proved. That is, in Eq. (23) below, the impulse response corresponding to a velocity profile as in Eq. (8) is given, for any $t > 0$ and any field point $\underline{r}$ (see Fig. 1) explicitly as a series involving the expansion coefficients u_n and certain functions $T^0_{2n}(t; \underline{r})$ given in finite terms in Eq. (24).

We have for the impulse response $h(t; \underline{r})$ in Eq. (4) that

$$h(t; \underline{r}) = \frac{c}{\pi} H(ct - z) \sum_{n=0}^{\infty} u_n T^0_{2n}(t; \underline{r}), \tag{10}$$

where T^0_{2n} is defined as

$$T^0_{2n}(t; \underline{r}) = \int_0^A R^0_{2n}[(w^2 + R^2 - 2wR \cos \alpha)^{1/2}/a]d\alpha$$
$$= \int_0^A P_n\left(2\frac{w^2 + R^2}{a^2} - 1 - \frac{4wR}{a^2}\cos \alpha\right)d\alpha. \tag{11}$$

Here, we recall the definitions of R and A in Eqs. (6), (7), and (9). Thus, in particular, T^0_{2n} vanishes when $|w - R| > a$.

The integral T^0_{2n} in Eq. (11) can be evaluated using the addition theorem for the Legendre polynomials, see Ref. 14, Sec. 220, pp. 364–371, in the form

$$P_n(\cos \gamma \cos \gamma' - \sin \gamma \sin \gamma' \cos \alpha)$$
$$= P_n(\cos \gamma)P_n(\cos \gamma') + 2\sum_{m=1}^{n}(-1)^m \frac{(n - m)!}{(n + m)!}$$
$$\times P_n^m(\cos \gamma)P_n^m(\cos \gamma')\cos m\alpha, \tag{12}$$

with real γ and γ' or

$$P_n(\mu\mu' - \sqrt{\mu^2 - 1}\sqrt{\mu'^2 - 1}\cos \alpha)$$
$$= P_n(\mu)P_n(\mu') + 2\sum_{m=1}^{n}(-1)^m \frac{(n - m)!}{(n + m)!}P_n^m(\mu)$$
$$\times P_n^m(\mu')\cos m\alpha, \tag{13}$$

with complex μ and μ' such that $\text{Re}(\mu), \text{Re}(\mu') > 0$ and $\mu, \mu' \notin (-\infty, 1]$. The P_n^m are the Legendre functions, see Ref. 13, Chap. 8.

In the case that $w + R < a$, Eq. (12) is used. In Appendix B, it is shown that

$$\cos \gamma \cos \gamma' = 2\frac{w^2 + R^2}{a^2} - 1, \quad \sin \gamma \sin \gamma' = \frac{4wR}{a^2} \tag{14}$$

holds when $\gamma, \gamma' \in (0, \pi)$ are given by

$$\cos(\gamma + \gamma') = 2\left(\frac{w - R}{a}\right)^2 - 1,$$
$$\cos(\gamma - \gamma') = 2\left(\frac{w + R}{a}\right)^2 - 1. \tag{15}$$

By Eq. (7), there holds $A = \pi$ in this case. Integration of Eq. (12) over $\alpha \in [\gamma, \pi]$ then yields

$$T^0_{2n}(t; \underline{r}) = \pi P_n(\cos \gamma)P_n(\cos \gamma'). \tag{16}$$

In terms of w, R, and a there holds

$$\cos \gamma = uv - (1 - u^2)^{1/2}(1 - v^2)^{1/2},$$
$$\cos \gamma' = uv + (1 - u^2)^{1/2}(1 - v^2)^{1/2} \tag{17}$$

with $u = |w - R|/a$, $v = (w + R)/a$.

In the case that $|w - R| < a < w + R$, Eq. (13) is used. In Appendix B, it is shown that

$$\mu\mu' = 2\frac{w^2 + R^2}{a^2} - 1, \quad \sqrt{\mu^2 - 1}\sqrt{\mu'^2 - 1} = \frac{4wR}{a^2} \tag{18}$$

is satisfied with $\text{Re}(\mu)$, $\text{Re}(\mu') > 0$ and $\mu, \mu' \notin (-\infty, 1]$ when

$$\mu = (\mu')^* = \cos \frac{1}{2}(\gamma_1 + i\gamma_2), \tag{19}$$

where $\gamma_1 \in (0, \pi)$, $\gamma_2 > 0$ are given by

$$\gamma_1 = \arccos\left[2\left(\frac{w - R}{a}\right)^2 - 1\right],$$
$$\gamma_2 = \text{arccosh}\left[2\left(\frac{w + R}{a}\right)^2 - 1\right]. \tag{20}$$

By Eq. (7), there holds $A \in (0, \pi)$ in this case. Integration of Eq. (13) over $\alpha \in [0, A]$, using that $P_n^m(\mu') = (P_n^m(\mu))^*$ yields

$$T^0_{2n}(t; \underline{r}) = A\left[|P_n(\mu)|^2 + 2\sum_{m=1}^{n}(-1)^m \frac{(n - m)!}{(n + m)!}\right.$$
$$\left. \times |P_n^m(\mu)|^2 \text{sinc}(mA)\right]. \tag{21}$$

In terms of w, R, and a there holds (u and v as above)

$$\mu = uv - i(1 - u^2)^{1/2}(v^2 - 1)^{1/2}. \tag{22}$$

Summarizing, there holds for $t > 0$ and field point $\underline{r}$

$$h(t; \underline{r}) = \frac{c}{\pi} H(ct - z) \sum_{n=0}^{\infty} u_n T^0_{2n}(t; \underline{r}), \tag{23}$$

where

$$T^0_{2n}(t; \underline{r}) = \begin{cases} 0 & , |w - R| > a, \\ \pi P_n(\cos \gamma)P_n(\cos \gamma') & , w + R < a, \\ \text{right-hand side of Eq. (21)} & , |w - R| < a < w + R, \end{cases} \tag{24}$$

with $R = (c^2t^2 - z^2)^{1/2} = R(t; z) > 0$ and $\gamma, \gamma' \in (0, \pi)$ given in case that $w + R < a$ by Eq. (17) while A, μ in case that $|w - R| < a < w + R$ are given by Eqs. (7) and (22).

The computation scheme is presented concisely in Appendix C where also a Mathematica code is supplied for the purpose of plotting impulse responses for a fixed value of z as a function of t and w

IV. DISCUSSION AND APPLICATION OF THE MAIN RESULT

The computation of impulse responses can be done using the following steps:

(1) Expand the radially symmetric velocity profile v into a (possibly infinite, appropriately truncated) Zernike series using expansion coefficients u_n as in Eq. (8).
(2) Compute the contribution to the impulse response of each Zernike term as a finite series according to Eq. (24).
(3) Form the linear combination of these contributions using the u_n as coefficients.

Feasibility of this approach depends critically on availability and rapid decay of the coefficients u_n in the expansion of Eq. (8) for the velocity profile of interest. As a first example, consider for $\ell = 0, 1, \cdots$ the parabolic profiles

$$v(\sigma) = v^{(\ell)}(\sigma) = (\ell + 1)V_s(1 - \sigma^2/a^2)^{\ell}H(a - \sigma). \quad (25)$$

There is the finite expansion, see Ref. 8, Appendix A1,

$$v^{(l)}(\sigma) = V_s \sum_{n=0}^{l} u_n^{(l)} R_{2n}^0(\sigma/a), \quad 0 \le \sigma \le a, \quad (26)$$

where

$$u_n^{(l)} = (-1)^l(2n+1)\binom{l+1}{n+1}\Big/\binom{l+n+1}{n+1},$$
$$l = 0, 1, \ldots, n. \quad (27)$$

Accordingly, the result of Greenspan in Ref. 11, Sec. VI, where the $v^{(l)}$ with $l = 0, 1, 2$ are considered, can be generalized in finite terms.

Similarly, for the monomial profiles, see Ref. 8, Appendix A1,

$$w^{(l)}(\sigma) = (l+1)W_s(\sigma^2/a^2)^l H(a - \sigma), \quad l = 0, 1, \ldots, \quad (28)$$

there is the expansion

$$w^{(l)}(\sigma) = W_s \sum_{n=0}^{l} (-1)^l u_n^{(l)} R_{2n}^0(\sigma/a), \quad 0 \le \sigma \le a, \quad (29)$$

where the $u_n^{(l)}$ are given in Eq. (27). Hence, the $w^{(l)}$ have impulse responses that can be computed in finite terms. Thus, when we have a profile of the form

$$v(\sigma) = V_s f((\sigma/a)^2)H(a - \sigma), \quad (30)$$

where $f(x)$ has a convergent Taylor series $\sum_{l=0}^{\infty} a_l x^l$, $|x| \le 1$, the impulse response of $v(\sigma)$ can be obtained, in principle, by linear combination of those of the $w^{(l)}$ in Eq. (29).

As a next example, consider the truncated Gaussian

$$v(\sigma; b) = \frac{bV_s}{1 - e^{-b}} e^{-b(\sigma/a)^2} H(a - \sigma), \quad (31)$$

for which there is the expansion, see Ref. 8, Appendix A2,

$$v(\sigma; b) = V_s \sum_{n=0}^{\infty} u_n(b)R_{2n}^0(\sigma/a), \quad 0 \le \sigma \le a, \quad (32)$$

with

$$u_n(b) = (-1)^n(2n+1)\frac{b/2}{\sinh(b/2)}\sqrt{\frac{\pi}{b}}I_{n+1/2}(b/2),$$
$$n = 0, 1, \ldots, \quad (33)$$

where I denotes the modified Bessel function, see Ref. 13, Sec. 9.6. In Ref. 11, Sec. VI C, Greenspan considers a non-truncated Gaussian (i.e., the piston has infinite radius a) and derives a formula, also involving the modified Bessel function, for the impulse response. Due to this different truncation strategy, this result is naturally different from what is obtained via the approach of the present paper. See Fig. 2 for the spatial impulse responses for: (a) a Gaussian velocity profile ($b = 4$), similar to Harris' Fig. 5(c) (see Ref. 3), using only nine terms in the Zernike expansion in Eq. (32) as explained and detailed in Appendix C; (b) for a rigid piston ($u_n = 0$ for $n \ne 0$ and $u_0 = 1$); and (c) for a simply supported radiator ($u_n = 0$ for $n > 1$ and $u_0 = 1$, $u_1 = -1$). In these plots, $z = \frac{1}{2}a$ is fixed and $\frac{1}{c}h(t; \underline{r})$ is displayed as a function of the normalized variables ct/a and w/a in the range $[0,2.5] \times [0,1.5]$.

There are many more velocity profiles of the type as in Eqs. (26), (29), and (32) allowing an explicit form for their Zernike expansion coefficients. Among these are the to $[0, a]$ truncated Bessel functions, sinc functions, and cosines.

The decay of the Zernike coefficients is determined by the smoothness properties of the velocity profile on the piston. For instance, see Ref. 8, Appendix A2, the truncated Gaussian in Eq. (31) has coefficients $u_n(b)$ that are significantly $\ne 0$ for integers n ranging from 0 to a little over $\frac{1}{2}eb$, after which very rapid decay occurs. Thus, the number of significant coefficients grows linearly with the parameter b which quantifies the spikiness of $v(\sigma; b)$ at $\sigma = 0$. It is furthermore noted that all T_{2n}^0 are bounded in modulus by π. This follows from Eq. (11), the fact that $0 \le A \le \pi$, and Ref. 13, Sec. 22.14.7 on p. 786, which shows that $|P_n(x)| \le 1$, $|x| \le 1$.

The method used by Stepanishen in Ref. 7, Sec. II, is next compared with the method in the present paper. Stepanishen uses Bessel functions $J_0(\alpha_j \sigma/a)$ as basis functions where $\alpha_0 = 0$ and $\alpha_1, \alpha_2, \ldots$ are the positive zeros of J_0. These functions yield orthogonal expansions for velocity profiles $v(\sigma)$ of the type as considered in Eq. (30) according to

$$v(\sigma) = V_s \sum_{j=0}^{\infty} s_j J_0(\alpha_j \sigma/a), \quad 0 \le \sigma \le a, \quad (34)$$

where $s_0 = 1$ and

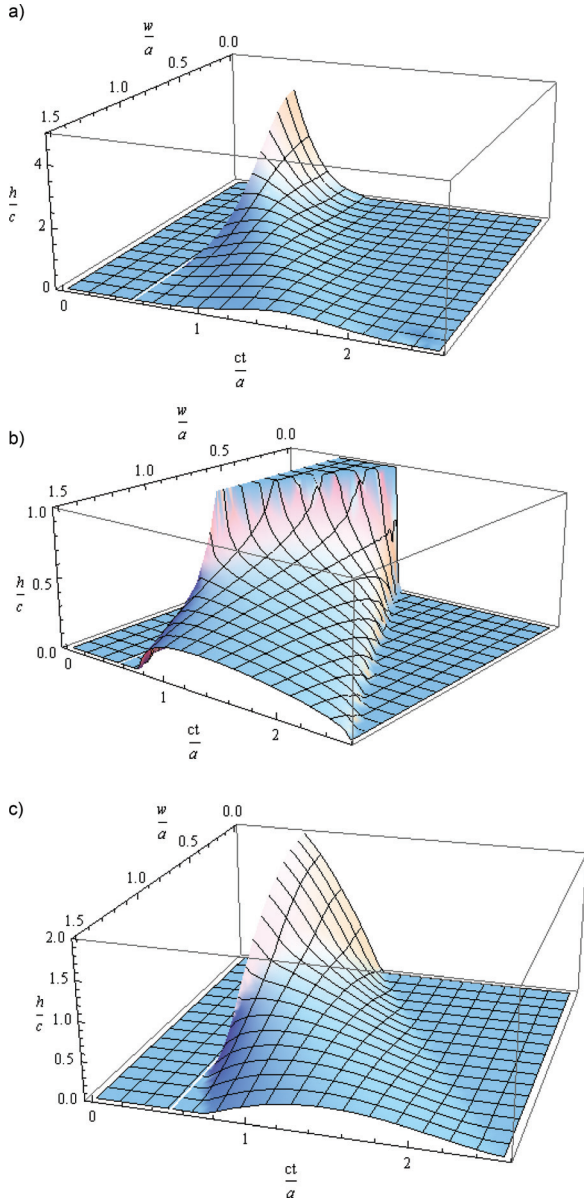$$s_j = \frac{2}{J_1^2(\alpha_j)} \int_0^1 f(\rho^2)J_0(\alpha_j \rho)\rho \, d\rho \quad (35)$$

J. Acoust. Soc. Am., Vol. 129, No. 5, May 2011

R. M. Aarts and A. J. Janssen: Spatial impulse responses   2955

FIG. 2. (Color online) Spatial impulse response for (a) Gaussian velocity profile ($b = 4$), (b) rigid piston case ($u_0 = 1$) $\ell = 0$ in Eq. (25), and (c) simply supported radiator, case ($u_0 = 1$, $u_1 = -1$) $\ell = 1$ in Eq. (25).

for $j = 1, 2, \ldots$, see Ref. 13, Sec. 11.4.1–5 on p. 485. Using Graf's addition theorem for Bessel functions, see Ref. 13, Sec. 9.1.79 on p. 363, the impulse response arising from a single Bessel term $J_0(\alpha_j \sigma/a)$ in accordance with Eq. (4) is expressed in Ref. 7 as

$$\frac{cA}{\pi} \sum_{m=-\infty}^{\infty} J_m(\alpha_j w) J_m(\alpha_j R(t;z)) \mathrm{sinc}(m\alpha_j A). \tag{36}$$

The series in Eq. (36) is infinite while the one for T_{2n}^0, see Eqs. (24) and (21), has at most $n + 1$ terms. The convergence properties of series of the type in Eq. (36) are quite well understood, however. The terms in the series in Eq. (36) are significantly $\neq 0$ for integers m for which $|m|$ ranges from 0 to a little over $\frac{1}{2}e\alpha_j \min \{w, R(t;z)\}$ after which very rapid decay occurs, see Ref. 13, Sec. 9.3.1 on p. 365. Note also that $\alpha_j \approx (j - \frac{1}{4})\pi$, $j = 1, 2, \ldots$ by Ref. 13, Sec. 9.5.12 on

p. 371, and this increases linearly in j. So, the convergence matter of the series in Eq. (36) requires some, but modest, care.

A second point is that the computation in analytic form of the coefficients s_j in Eq. (35) is cumbersome (except in the case that $v(\sigma)$ is a finite linear combination of the $J_0(\alpha_j \sigma/a)$). In the case of polynomial profiles $v(\sigma)$, a finite-terms expression, using repeated partial integrations with $z^r J_{r-1}(z) dz = d[z^r J_r(z)]$, see Ref. 13, Sec. 9.1.30 on p. 361, can be derived, but this is already quite complicated. Moreover, even in this case, infinitely many s_j are non-vanishing. In the case of the truncated Gaussian profile, see Eq. (31), complicated special functions like the Lommel functions of two variables, see Ref. 15, Sec. 16.5 on pp. 537–550, appear.

An even more serious problem is the fact that the expansion coefficients s_j in Eq. (35) decay slowly, also in cases of very well-behaved profiles $v(\sigma)$. With $v(\sigma)$ of the form in Eq. (30) and K the smallest non-negative integer such that $f^{(K)}(1) \neq 0$, the leading behavior of s_j as j gets large is given by

$$\frac{1}{\alpha_j J_1^2(\alpha_j)} \left(\frac{-2}{\alpha_j}\right)^K f^{(K)}(1) J_{K+1}(\alpha_j). \tag{37}$$

This follows from repeated partial integrations in Eq. (35) using $z^r J_{r-1}(z) dz = d[z^r J_r(z)]$ as above for the polynomial profiles. Thus for a Gaussian profile as in Eq. (31), for which we have that $f(x)$ is a multiple of $\exp(-bx)$, there holds $K = 0$ in Eq. (37) and decay is only as slow as $j^{-1/2}$ as $\alpha_j \approx (j - \frac{1}{4})\pi$ and $J_1(\alpha_j) \approx (-1)^{j-1} j^{1/2}/\pi$, see Ref. 13, Sec. 9.5.12 on p. 371 and Sec. 9.2.1 on p. 364. Also compare with the discussion at the end of Ref. 12 where the Zernike expansion coefficients decay is compared with coefficients decay when $J_0(\beta_j \sigma/a)$, with $\beta_0 = 1$ and $\beta_1, \beta_2, \ldots$ the zeros of J_0', are used as expansion coefficients.

V. CONCLUSIONS AND OUTLOOK

Using Zernike expansions of radially symmetric velocity profiles on a baffled, circular piston, a computation scheme for spatial impulse responses has been presented. The impulse responses of the constituent basis functions $R_{2n}^0(\sigma/a) = P_n(2(\sigma/a)^2 - 1)$ have been computed explicitly as finite series involving the Legendre functions and the sinc function. The method has been compared in theory with the method introduced by P. R. Stepanishen that uses orthogonal Bessel functions instead of Zernike polynomials. Among the advantages of the method of this paper over Stepanishen's method are finite series results for impulse responses in the case of polynomial velocity profiles and better decay of expansion coefficients. This latter point is also instrumental when the method is used in the reverse direction so as to estimate velocity profiles in terms of expansion coefficients from the measured spatial responses. The authors intend to investigate this inverse method in more detail, including comparison with earlier approaches to acoustical holography.

An extension of the finite-series representation of impulse responses to non-radially symmetric basis functions $Z_n^m(\sigma, \varphi) = e^{im\varphi} P_{n-m/2}^{(0,m)}(2(\sigma/a)^2 - 1)$ is envisaged as well. These Z_n^m are the general Zernike circle polynomials as used

in the diffraction theory[17–19] of optical aberrations. In the case of non-radially symmetric velocity profiles, the impulse response $h(t; \underline{r})$ can still be expressed in terms of an integral of the velocity profile along an arc in the piston plane consisting of all points that are at the common distance ct from the field point $\underline{r}$. The generalization of the main result critically depends on the availability of an addition theorem to write the mentioned integral with profile Z_n^m in finite terms. Such an addition theorem is indeed available and can be established by using the approach in Ref. 16 on representing scaled and shifted Zernike circle polynomials.

ACKNOWLEDGMENTS

APPENDIX A: PROOF OF EQ. (4)

The (normalized) impulse response is the inverse Fourier transform of the velocity potential, that is,

$$h(t; \underline{r}) = \frac{1}{2\pi V_s} \int_{-\infty}^{\infty} e^{i\omega t} \phi(\underline{r}; \omega) d\omega \tag{A1}$$

with $\phi(\underline{r}; \omega)$ given in Eq. (3). Since v is radially symmetric, so is $\phi(\underline{r}; \omega)$ and the field point $\underline{r}$ can be taken to be $(w, 0, z)$. In the integral at the right-hand side of Eq. (3), polar coordinates $(x_s, y_s) = (w, 0) - R(\cos \alpha, \sin \alpha)$ are taken with the projection $(w, 0, 0)$ of the field point $\underline{r}$ on the piston plane as origin. Using

$$|\underline{r}_s| = (w^2 + R^2 - 2Rw \cos \alpha + z^2)^{1/2},$$
$$|\underline{r}_s - \underline{r}| = (R^2 + z^2)^{1/2}, \tag{A2}$$

it follows that

$$\phi(\underline{r}, \omega) = \frac{1}{2\pi} \int_0^\infty \int_0^{2\pi} v((w^2 + R^2 - 2Rw \cos \alpha)^{1/2})$$
$$\times \frac{e^{-ik(R^2 + z^2)^{1/2}}}{(R^2 + z^2)^{1/2}} R dR d\alpha. \tag{A3}$$

Next, the substitution $W = (R^2 + z^2)^{1/2} \geq z$ is made. Writing $R(W; z) = (W^2 - z^2)^{1/2}$ and using $RdR = WdW$, there results

$$\phi(r, \omega) = \frac{1}{2\pi} \int_z^\infty \int_0^{2\pi} v((w^2 + R^2(W; z)$$
$$- 2R(W; z) \cos \alpha)^{1/2}) e^{-ikW} dW d\alpha. \tag{A4}$$

Then performing inverse Fourier transformation in Eq. (A1) and recalling that $k = \omega/c$, it follows that

$$h(t, \underline{r}) = \frac{c}{2\pi V_s} \int_0^{2\pi} v((w^2 + R^2(ct; z)$$
$$- 2R(ct; z) \cos \alpha)^{1/2}) d\alpha H(ct - z). \tag{A5}$$

Here, it has been used that

$$\frac{1}{2\pi} \int_{-\infty}^{\infty} e^{i\omega t - i\omega W/c} d\omega = \delta(t - W/c) = c\delta(W - ct). \tag{A6}$$

The formula in Eq. (4), with A as given in Eq. (7), then follows from the fact that $v(\underline{r}_s)$ actually vanishes for $|\underline{r}_s| > a$ and some administration with inverse trigonometric functions.

APPENDIX B: LEGENDRE FUNCTIONS AND ADDITION FORMULA

There holds, see Ref. 13, Sec. 8.6.6–7 on p. 334, for integer n, m with $0 \leq m \leq n$ that

$$P_n^m(x) = (-1)^n (1 - x^2)^{\frac{1}{2}m} \frac{d^m P_n(x)}{dx^m}, \quad -1 < x < 1, \tag{B1}$$

and

$$P_n^m(z) = (z^2 - 1)^{\frac{1}{2}m} \frac{d^m P_n(z)}{dz^m}, \quad \text{Re } z > 0, \quad z \notin (-\infty, 1], \tag{B2}$$

where P_n is the Legendre polynomial of degree n and where the principal values of the square roots are taken in Eqs. (B1) and (B2).

The two conditions in Eq. (14) are equivalent to the two conditions in Eq. (15) by the addition theorem for cos. Since $w + R < a$ by assumption and w, $R > 0$ there holds $2(w \pm R/a)^2 - 1 \in (-1, 1)$ and so Eq. (15) is satisfied with γ, γ' satisfying $0 < \gamma' \leq \gamma < \pi$ and given by $\frac{1}{2}(\alpha_- \pm \alpha_+)$ where

$$\alpha_\pm = \arccos\left(2\left(\frac{w \pm R}{a}\right)^2 - 1\right) \in (0, \pi). \tag{B3}$$

Then $\cos \gamma$, $\cos \gamma'$ can be computed from $\cos \frac{1}{2}(\alpha_- \pm \alpha_+)$ using the addition theorem for cos and $\cos \frac{1}{2}\alpha = (\frac{1}{2}(1 + \cos \alpha))^{1/2}$, $\sin \frac{1}{2}\alpha = (\frac{1}{2}(1 - \cos \alpha))^{1/2}$ when $0 < \alpha < \pi$, and this yields Eq. (17).

In the case that $|w - R| < a < w + R$, there holds

$$2\left(\frac{w - R}{a}\right)^2 - 1 \in (-1, 1), \quad 2\left(\frac{w + R}{a}\right)^2 - 1 > 0, \tag{B4}$$

and so γ_1, γ_2 in Eq. (20) can be taken such that $\gamma_1 \in (0, \pi)$, $\gamma_2 > 0$. Therefore, $\cos \frac{1}{2}\gamma_1$, $\sin \frac{1}{2}\gamma_1$, $\cosh \frac{1}{2}\gamma_2$, and $\sinh \frac{1}{2}\gamma_2$ are all positive so that μ and μ' in Eq. (19) satisfy Re μ, Re $\mu' > 0$ and μ, $\mu' \notin (-\infty, 1]$ by the addition theorem for cos. Letting $\gamma = \frac{1}{2}(\gamma_1 + i\gamma_2)$, it follows from $\mu' = \mu^*$ that

$$\mu\mu' = \cos \gamma \cos \gamma^*, \quad \sqrt{\mu^2 - 1}\sqrt{\mu'^2 - 1} = \sin \gamma \sin \gamma^* \tag{B5}$$

(positive numbers at both sides at either equality). By the addition theorem for cos it is then seen that

$$\mu\mu' + \sqrt{\mu^2 - 1}\sqrt{\mu'^2 - 1} = \cos(\gamma - \gamma^*)$$
$$= \cosh \gamma_2$$
$$= 2\left(\frac{w + R}{a}\right)^2 - 1, \tag{B6}$$

$$\mu\mu' - \sqrt{\mu^2 - 1}\sqrt{\mu'^2 - 1} = \cos(\gamma + \gamma^*)$$
$$= \cos\gamma_1$$
$$= 2\left(\frac{w - R}{a}\right)^2 - 1, \qquad \text{(B7)}$$

and it follows that the two conditions in Eq. (18) are satisfied. Finally, the equality in Eq. (22) follows in a similar fashion as the equalities in Eq. (17) were proved.

APPENDIX C: COMPUTATION SCHEME FOR PLOTTING $h(t; r)$

With $t > 0$ and $\underline{r} = (w, 0, z)$ set

$$x_a = w/a, \quad y_a = ct/a, \quad z_a = z/a, \quad r_a = (y_a^2 - z_a^2)^{1/2}.$$
$$\text{(C1)}$$

Assume that in good approximation

$$v(\sigma) = V_s \sum_{n=0}^{N} u_n R_{2n}^0(\sigma/a). \qquad \text{(C2)}$$

Then in good approximation

$$h(t; \underline{r}) \equiv h(x_a, y_a, z_a)$$
$$= \frac{c}{\pi} H(y_a - z_a) \sum_{n=0}^{N} u_n T_{2n}(x_a, y_a, z_a) \qquad \text{(C3)}$$

where H is the Heaviside function and

$$T_{2n}(x_a, y_a, z_a) = \begin{cases} 0 & , u > 1, \\ \pi P_n(uv - (1 - u^2)^{1/2}(1 - v^2)^{1/2}) P_n(uv + (1 - u^2)^{1/2}(1 - v^2)^{1/2}) & , v < 1, \\ A\left[|P_n(\mu)|^2 + 2\sum_{m=1}^{n} (-1)^m \frac{(n-m)!}{(n+m)!}|P_n^m(\mu)|^2 \text{sinc}(ma)\right] & , u < 1 < v, \end{cases} \qquad \text{(C4)}$$

with $u = |x_a - r_a|, v = |x_a + r_a|$ and

$$A = \arccos\left[\frac{x_a^2 + r_a^2 - 1}{2x_a r_a}\right],$$
$$\mu = uv - i(1 - u^2)^{1/2}(v^2 - 1)^{1/2}. \qquad \text{(C5)}$$

For the case that $v(\sigma)$ is given by Eq. (32) with $b = 4$ and $V_s = 1$ m/s, one can take $N = 8$ in Eq. (C2) (relative error $\leq 0.001\%$), and the $u_n(b)$ are given by

$$u_n(b) = (-1)^n (2n + 1) \frac{b/2}{\sinh(b/2)} \left(\frac{\pi}{b}\right)^{1/2} I_{n+1/2}(b/2),$$
$$n = 0, 1, \cdots, 8. \qquad \text{(C6)}$$

This results for Fig. 2(a) in the following Mathematica code.

```
u[n_, b_] := (-1) ^n (2 n+1) b/2/Sinh[b/2]
Sqrt[Pi/b] BesselI[n+1/2, b/2]
b=4
h[x_, y_, z_] := c/Pi UnitStep [y - z]
Sum[u[n, b] T2[n, x, y, z] , {n, 0, 8}]
T2[n_, x_, y_, z_] := Module[{u, v, r},
  r = Sqrt[y^2 - z^2] ; u = Abs [x - r] ; v = Abs
  [x + r] ;
  Which[u >= 1, 0,
  v <= 1,
  Pi LegendreP[n, u v - Sqrt[1 - u^2]  Sqrt
  [1 - v^2]] LegendreP[n,
   u v + Sqrt[1 - u^2] Sqrt [1 - v^2]],
  True,
```

```
With[{a = ArcCos[(x^2 + r^2 - 1)/(2 × r)],
  \[Mu] = u v - I Sqrt[1 - u^2] Sqrt[v^2 - 1]},
  a (Abs[LegendreP[n, \[Mu]]]^2 +
  2 Sum[(-1)^m (n - m)!/(n + m)! Abs
  [LegendreP[n, m, \[Mu]]]^2
  Sinc[m a], {m, 1, n}])]]]
Plot3D[h[x, y, 0.5]/c, {x, 0, 1.5}, {y, 0,
2.55}, PlotRange → {0, 5},
AxesLabel → {w/a, ct/a, h/c}]
```

[1]P. R. Stepanishen, "Transient radiation from pistons in an infinite planar baffle," J. Acoust. Soc. Am. **49**, 1629–1638 (1971).

[2]G. R. Harris, "Review of transient field theory for a baffled planar piston," J. Acoust. Soc. Am. **70**, 10–20 (1981).

[3]G. R. Harris, "Transient field of a baffled planar piston having an arbitrary vibration amplitude distribution," J. Acoust. Soc. Am. **70**, 186–204 (1981).

[4]J. A. Jensen, "A new calculation procedure for spatial impulse responses in ultrasound," J. Acoust. Soc. Am. **105**, 3266–3274 (1999).

[5]T. Otani, "Physical principles and theoretical concepts of transient acoustic field," Jpn. J. Appl. Phys. **39**, 2888–2897 (2000).

[6]R. J. McGough, T. V. Samulski, and J. F. Kelly, "An efficient grid sectoring method for calculations of the near-field pressure generated by a circular piston," J. Acoust. Soc. Am. **115**, 1942–1954 (2004).

[7]P. R. Stepanishen, "Acoustic transients from planar axisymmetric vibrators using the impulse response approach," J. Acoust. Soc. Am. **70**, 1176–1181 (1981).

[8]R.M. Aarts and A. J. E. M. Janssen, "On-axis and far-field sound radiation from resilient flat and dome-shaped radiators," J. Acoust. Soc. Am. **125**, 1444–1455 (2009).

[9]R.M. Aarts and A. J. E. M. Janssen, "Sound radiation quantities arising from a resilient circular radiator," J. Acoust. Soc. Am. **126**, 1776–1787 (2009).

[10]R.M. Aarts and A. J. E. M. Janssen, "Sound radiation from a resilient spherical cap on a rigid sphere," J. Acoust. Soc. Am. **127**, 2262–2273 (2010).

[11]M. Greenspan, "Piston radiator: Some extensions of the theory," J. Acoust. Soc. Am. **65**, 608–621 (1979).

[12]R.M. Aarts and A. J. E. M. Janssen, "Authors' Reply on comments on 'Estimating the velocity profile and acoustical quantities of a harmonically

vibrating loudspeaker membrane from on-axis pressure data'," J. Audio Eng. Soc. **58**, 308–310 (2010).

[13]M. Abramowitz and I. A. Stegun, *Handbook of Mathematical Functions* (Dover, New York, 1972), pp. 331–786.

[14]E. W. Hobson, *The Theory of Spherical and Ellipsoidal Harmonics* (Cambridge University Press, Cambridge, 1955), pp. 364–371.

[15]G. N. Watson, *A Treatise on the Theory of Bessel Functions* (Cambridge University Press, Cambridge 1944), pp. 411–415, 537–550.

[16]A. J. E. M. Janssen, "Zernike circle polynomials and infinite integrals involving the product of Bessel functions," arXiv:1007.0667v1, July 5 2010, also available from the Eindhoven University of Technology Library, ISBN: 978-90-386-2290-3.

[17]F. Zernike, "Diffraction theory of the knife-edge test and its improved version, the phase-contrast method (published in German as Beugungstheorie des Schneidenverfahrens und seiner verbesserten Form, der Phasenkontrastmethode)," Physica **1**, 689–704 (1934).

[18]B. R. A. Nijboer, "The diffraction theory of aberrations." Ph.D. dissertation, University of Groningen, The Netherlands, 1942.

[19]M. Born and E. Wolf, *Principles of Optics*, 7th ed. (Cambridge University Press, Cambridge, 2002), Chap. 9.